2009 International Symposium on Nonlinear Theory and its Applications
NOLTA'09, Sapporo, Japan, October 18-21, 2009

A Simplified Region-based Coupled MRF Model for Coarse Image Region Segmentation toward Its VLSI Implementation

Kenji Matsuzaka and Takashi Morie

Graduate School of Life Science and Systems Engineering, Kyushu Institute of Technology
2-4, Hibikino, Wakamatsu-ku, Kitakyushu, 808-0196 Japan
Email: matsuzaka-kenji@edu.brain.kyutech.ac.jp, morie@brain.kyutech.ac.jp

Abstract—This paper proposes a simplified region-based coupled Markov Random Field (MRF) model for coarse image region segmentation. We previously simplified the region-based MRF model with hidden phase variables for the same purpose, and proposed its VLSI implementation. However, the model was still complicated and the layout area of its VLSI circuit was still large. In this paper, we propose a further simplified model by using piecewise binary functions, and demonstrate its superior performance to our previous model by numerical simulations.

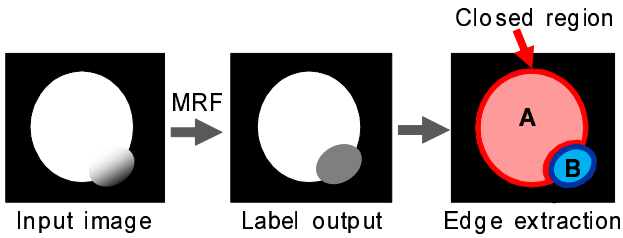

Figure 1: Image region segmentation by region-based coupled MRF model.

1. Introduction

On the Basis of visual computational theories, coupled Markov Random Field (MRF) models provide practical algorithms and hardware implementation for detecting discontinuities in motion, intensity, color, and depth in image scenes [2–6]. In the region-based coupled MRF models, hidden variables represent a label process. The hidden variables play a crucial role in detecting the discontinuities. Even if an input image contains gradations, the region-based models can extract closed regions from the input image by a label process as shown in Fig. 1.

However, the region-based coupled MRF model has a problem that solutions obtained from the gradient descending method are often trapped in local minima. In order to overcome this problem, a region-based coupled MRF model with hidden phase variables was proposed, and it is shown that the neutral stability of the phase variables settles a steady state at a global minimum [7].

We proposed the improved region-based coupled MRF model with hidden phase variables for efficient coarse image region segmentation and its VLSI implementation [8]. We designed a merged analog/digital CMOS circuit implementing this model. However, the layout area of this CMOS circuit is still large. Therefore, it is necessary to simplify this model.

In this paper, we simplify and improve this model toward its VLSI implementation, and apply it to the coarse image region segmentation task. We show performance comparison results with our previous model [8].

2. Region-based coupled MRF models

2.1. Region-based coupled MRF model with hidden phase variables

The coupled MRF model employs mutual coupling of the intensity and label processes as shown in Fig. 2. The interaction is achieved using the differences between state values of neighboring pixels. The cost function of this model is represented as follows [7]:

$$\begin{aligned} E(f,\phi,d) &= \frac{1}{2}\sum_i (f_i - d_i)^2 \\ &\quad + \frac{\lambda}{4}\sum_i \{1+\cos(\Delta\phi)\}(\Delta f)^2 \\ &\quad - \frac{J}{2}\sum_i \cos(\Delta\phi), \\ \Delta\phi &= \phi_j - \phi_i, \\ \Delta f &= f_j - f_i \end{aligned} \tag{1}$$

where f_i is the state value at the i-th node referred to as the intensity process, ϕ_i is the phase as hidden variables referred to as a label process, d_i the input value at the i-th node, and λ and J the scale parameters.

In Eq. (1), the first term forces f_i to be close to d_i. The second term smoothes the gradient between f_i and f_j according to the difference between the corresponding phase variables. Phase variable ϕ_i also interacts with neighboring phase variables and the corresponding state f_i. The third term is the constraint with respect to the phase variables.

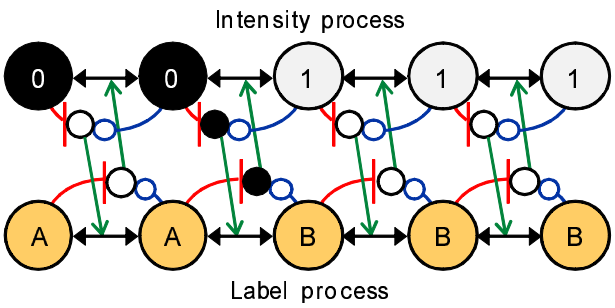

Figure 2: Neural network model of the region-based MRF.

The discretized algorithm for minimizing the cost function is represented as follows:

$$f_i(t+1) = f_i(t) + \sum_i \varepsilon_f \left[\lambda \left\{ \frac{1+\cos(\Delta\phi)}{2} \right\} \Delta f - (f_i - d_i) \right], \quad (2)$$

$$\phi_i(t+1) = \phi_i(t) + \sum_i \frac{\varepsilon_\phi}{2} \left\{ J - \frac{\lambda}{2} (\Delta f)^2 \right\} \sin(\Delta\phi) \quad (3)$$

where ε_f and ε_ϕ are constants.

2.2. Our previous (old) model

In the above-mentioned model, it is difficult to optimize the parameters λ and J, which determine the balance between image segmentation and smoothing, because the coefficient of the second term in Eq. (3) is a quadratic function of Δf. To overcome this problem, we previously proposed an improved model [8]. The updating equations of this model is described as follows:

$$f_i(t+1) = f_i(t) + \sum_i \frac{h_f}{4} \left[\frac{1+\cos(\Delta\phi)}{2} B - 4\eta(f_i - d_i) \right], \quad (4)$$

$$\phi_i(t+1) = \phi_i(t) + \sum_i \frac{h_\phi}{4} \pi A \sin(\Delta\phi) \quad (5)$$

where h_f, h_ϕ, and η are constants, and coefficients A and B are given by:

$$A = \begin{cases} -1 & \text{if } Q < \Delta f \le 1 \\ 1 & \text{if } -Q \le \Delta f \le Q \\ -1 & \text{if } -1 \le \Delta f < -Q \end{cases}$$

$$B = \begin{cases} 1 & \text{if } 0 < \Delta f \le 1 \\ 0 & \text{if } \Delta f = 0 \\ -1 & \text{if } -1 \le \Delta f < 0 \end{cases}$$

where Q is the parameter that determines whether segmentation or smoothing is dominant in the label process. The piecewise binary coefficients are suitable for practical hardware implementation.

It has been confirmed by numerical simulation of the coarse image region segmentation task that this model is superior to the original one expressed by Eqs. (2) and (3). This model has the features that the number of clustered regions is controlled by parameter Q, and that the image is not clustered into too small regions.

2.3. Proposed (new) model

In hardware implementation, our previous model is still complicated because both intensity and label processes are expressed by the nonlinear functions. Therefore, we change these nonlinear functions to piecewise binary functions.

In the updating equations of our previous model expressed by Eqs. (4) and (5), both $\sin(\Delta\phi)$ and $(1+\cos(\Delta\phi)/2$ are nonlinear. Instead of these functions, we use functions S and C, respectively, as shown in Fig. 3.

Here, we set intervals α and β around the convergence and divergence points. The updating amounts become zero in these regions, so that the processes can be settled to the steady state. The spatial resolution of both intensity and label processes does not have to be high, because our previous model has features that the image is not divided into too small regions. Therefore, we assumed that the introduction of intervals α and β do not have a bad effect on the processing results.

Next, we delete unnecessary terms in the updating equations of our previous model. In coarse image region segmentation tasks, the intensity process does not necessarily correspond to the input image pixel data. In fact, parameter η that determines this effect is very small compared with other terms in the previous model. Therefore, we set $\eta = 0$ in Eq. (4).

Based on these simplifications, we propose a new region-based coupled MRF model. The updating equations in our

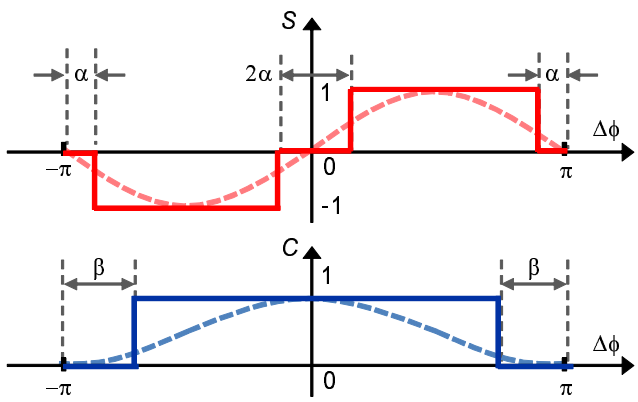

Figure 3: Simplified functions S and C.

proposed model are described as follows:

$$f_i(t+1) = f_i(t) + \sum_i \frac{h_f}{4} CB, \tag{6}$$

$$\phi_i(t+1) = \phi_i(t) + \sum_i \frac{h_\phi}{4} \pi AS, \tag{7}$$

Coefficients A and B are the same as those in our previous model, and functions S and C are given by:

$$S = \begin{cases} 1 & \text{if } \alpha \le \Delta\phi \le \pi - \alpha \\ -1 & \text{if } -\pi + \alpha \le \Delta\phi \le -\alpha \\ 0 & \text{otherwise} \end{cases}$$

$$C = \begin{cases} 1 & \text{if } -\pi + \beta \le \Delta\phi \le \pi - \beta \\ 0 & \text{otherwise} \end{cases}$$

The values of intervals α and β depend on the coefficients of the updating amounts and the processing resolution. The piecewise binary functions S and C (Fig. 3) as well as A and B make the practical hardware implementation easier.

3. Numerical simulation results

We compared the performance of the new model proposed in this paper and our previous (old) model by numerical simulation.

3.1. Gradient limits in geometric figure

We evaluated the performance of the new model for detection of discontinuities in the label process in terms of gradient limits [5]. We used a geometric figure with a gradation as an input image, as shown in Fig. 4. We normalized input values d_i within [0,1] and set initial phases ϕ_i at πd_i. For comparison, we used the same parameters in both models except Q. We show the results in Fig. 4. We converted the values of the phase variables in the label process into hue.

In our old model, the gradation region is divided into regions whose number depends on parameter Q if $Q = 0.1$, 0.05 and 0.01. However, when $Q = 0.001$, the number of clustered regions is almost the same as that when $Q = 0.01$. Therefore, although the number of clustered regions is controlled by parameter Q, the gradient region is not divided into too small region even if Q is very small. In the new model, the results are nearly the same.

As a result, we confirmed that the controllability of gradient limits, which our old model has, still remains in the new model.

3.2. Number of iterative calculations for image restoration

We compared the performance of the new model and our old model in terms of the number of iterative calculations for image restoration (noise elimination) tasks. We used an input image in which noise is added to a geometric figure consisting of two regions, as shown in Fig. 5. We used the same parameters in both models, and found the number of iterations required for image restoration. The completion of image restoration is defined as the timing when the result of sobel filtering shows only the boundary of the two regions.

In our old model, the number of iterations required for image restoration is about 5,000. Even in that case, the edge of the boundary is not a straight line, which means that smoothing of small regions is insufficient.

In the new model, the number of iterations required for image restoration is about 300, which is more than ten times smaller than that in our old model. Furthermore, the

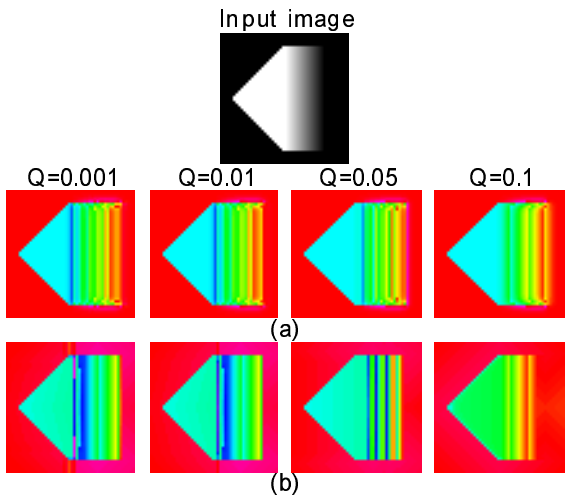

Figure 4: Detection of discontinuities in (a) our old model and (b) new model.

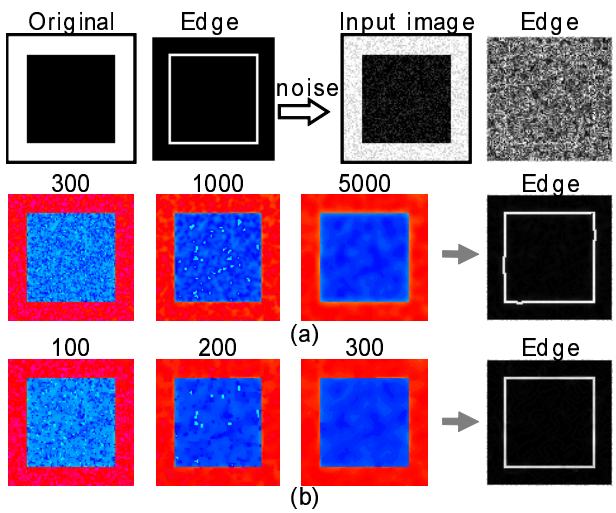

Figure 5: Iterations required for image restoration in (a) our old model and (b) new model.

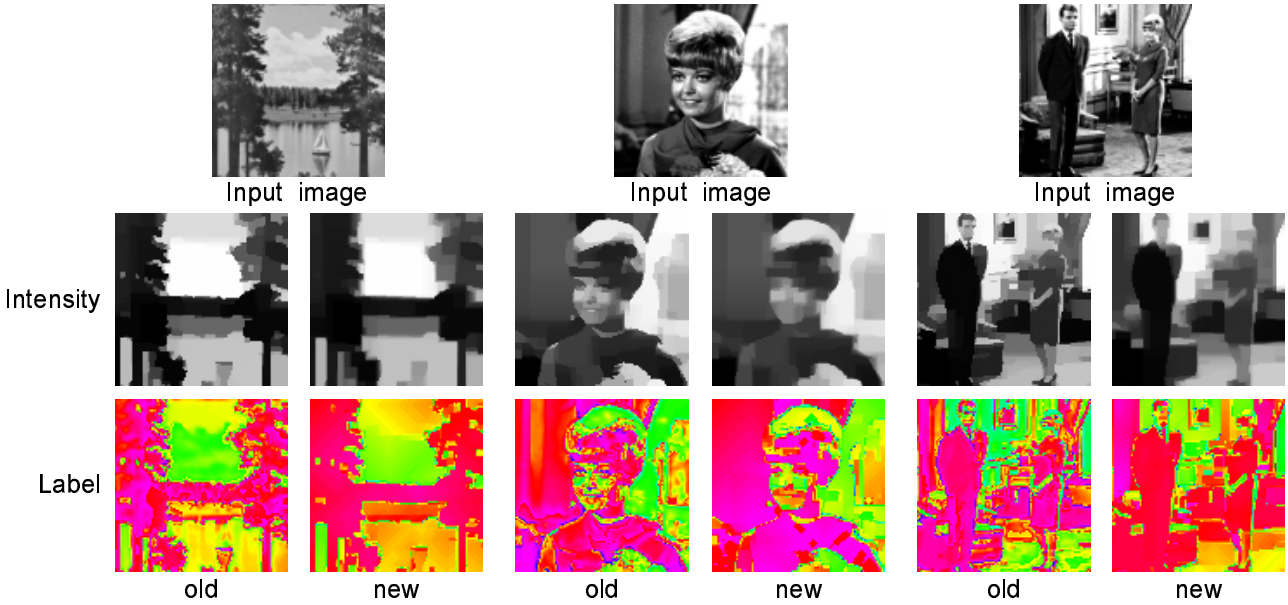

Figure 6: Coarse image region segmentation in various images.

edge of the boundary is a straight line, which indicates a superior image restoration ability.

These superior results are obtained from the feature that the updating amount is fixed to the maximum value by introducing the piecewise binary functions.

3.3. Coarse image region segmentation

We verified the coarse image region segmentation ability of the new model by using various images. We used pictures shown in Fig. 6, which are often used for benchmark tests in image processing. All the parameters are also the same in both models. From Fig. 6, as for smoothing within small regions, the new model is superior to our old model. Although the boundaries of the clustered regions in the intensity process are often blurred, those in the label process are clear, and therefore coarse region segmentation can successfully be achieved.

4. Conclusion

In this paper, we proposed a simplified region-based coupled MRF model with hidden phase variables toward its VLSI implementation, and apply it to the coarse image region segmentation. We changed the nonlinear functions to piecewise binary functions, and deleted unnecessary terms in the updating equations of our old model. We demonstrated from the numerical simulations that the proposed simplified model not only retains the advantages of our old model, but also improves the processing speed and the region segmentation ability. The proposed new model makes VLSI implementation easier because of the simplicity of the updating equations.

References

[1] D. Marr, *Vision*, W. H. Freeman and Co, New York, 1982.

[2] S. Geman and D. Geman, "Stochastic relaxation, Gibbs distributions, and the Bayesian restoration of images," *IEEE Trans. Pattern Anal. Mach. Intell.,* vol. 6, pp. 721-741, 1984.

[3] D. Geman, S. Geman, C. Graffigne, and P. Dong, "Boundary detection by constrained optimization," *IEEE Trans. Pattern Anal. Mach. Intell.,* vol. 12, pp. 609-628, 1990.

[4] C. Koch, J. Marooquin, and A. Yuille, "Analog "neuronal" networks in early vision," *Proc. National Academy of Sciences,* vol. 83, no. 12, pp. 4263-4267, 1986.

[5] A. Blake and A. Zisserman, *Visual Reconstruction*, MIT Press, Cambridge, MA, 1987.

[6] A. Lumsdaine, J. Waytt, and I. Elfadel, "Nonlinear analog networks for image smoothing and segmentation," *Proc. IEEE Int. Symp. on Circuits and Systems (ISCAS 1990)*, pp. 987-991, 1990.

[7] M. Okada, K. Doya, T. Yoshioka, and M. Kawato, "A region-based coupled MRF model with the phases as the hidden variables," *IEICE Technical Report*, vol. 98, no. 674, pp. 239-246, 1999.

[8] Y. Kawashima, D. Atuti, K. Nakada, M. Okada, and T. Morie, "Coarse Image Region Segmentation Using Region- and Boundary-based Coupled MRF Models and Their PWM VLSI Implementation",*Proc. Int. Joint Conf. on Neural Networks (IJCNN 2009)*, pp. 1559-1565, 2009.